Supplementary Materials for

Deciphering Relative Sea-Level Change in Chesapeake Bay: Impact of Global Mean, Regional Variation, and Local Land Subsidence, Part 1: Methodology

Yi Liu*, Xin Zhou

Morgan State University, Department of Civil & Environmental Engineering, Baltimore, MD 21251

Correspondence: yi.liu@morgan.edu

This PDF file includes:

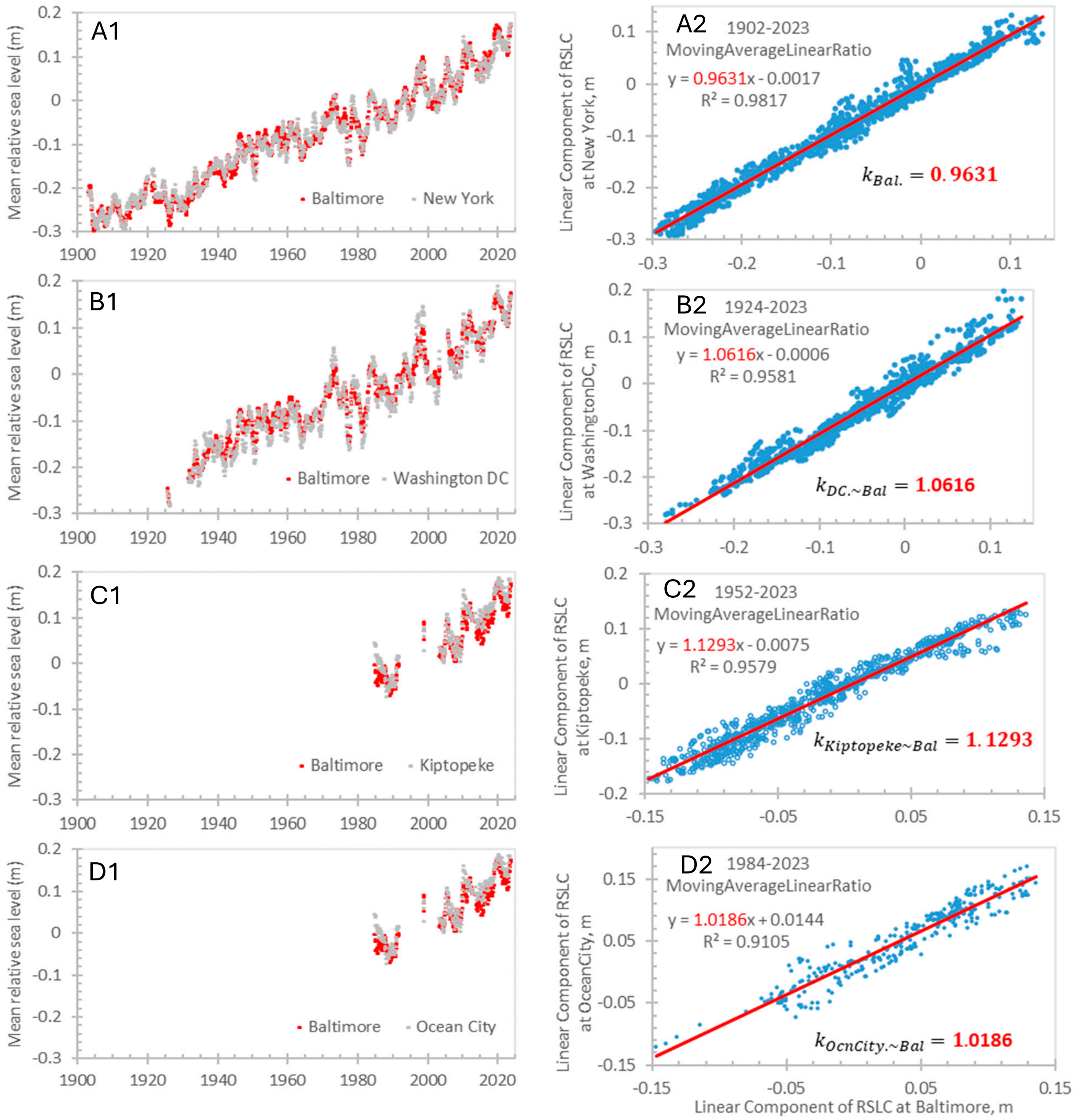

Supplementary Figure S1 The correlation of reformed 11-month moving average relative sea levels between tide gauge Baltimore and each of 14 short-term tide gauges. Each main chart shows reformed sea-level data by removing accelerated sea-level values using acceleration of 0.0991 mm/y^2 as shown in Fig. 6. Each sub-chart on the upper-left corner of its main chart shows their paired sea-level linear correlation with a linear equation and a squared correlation value. Each sub-chart on the lower-right corner of its main chart shows further paired sea-level correlation with a linear equation and a squared correlation value between the Baltimore and Battery New York tide gauges. Both linear coefficient values of $k_{tg\sim Bal}$ in B2 through O2 and $k_{NY\sim Bal}$ in A2 are given Table S4. **A1, A2.** New York and Baltimore itself; **B1, B2.** Washington D.C.; **C1, C2.** Ocean City; **D1, D2.** Kiptopeke; (continued)

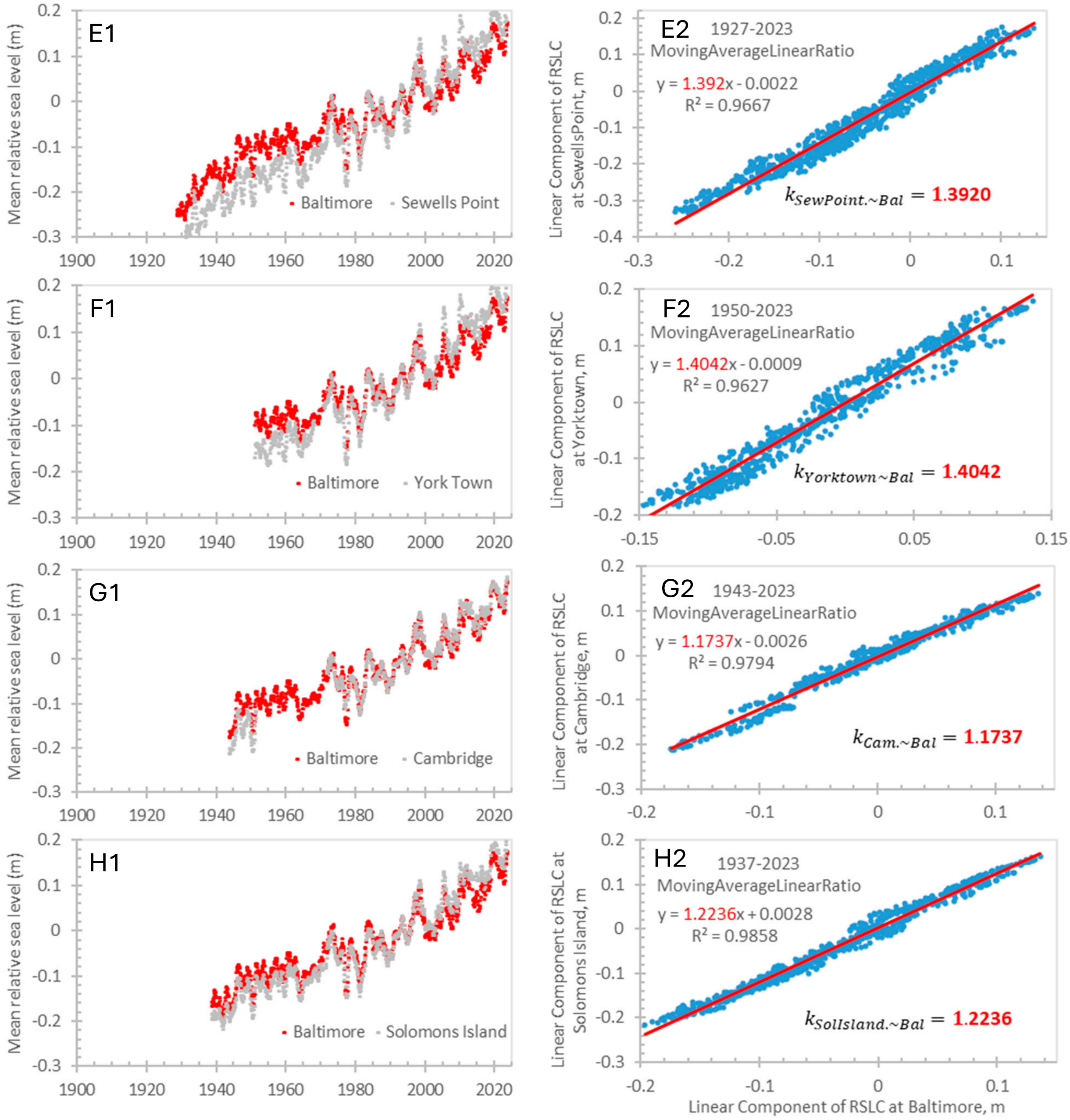

Supplementary Figure S1 (Continued) The correlation of reformed 11-month moving average relative sea levels between tide gauge Baltimore and each of 14 short-term tide gauges. **E1, E2.** Sewells Point; **F1, F2.** Yorktown; **G1, G2.** Cambridge; **H1, H2.** Solomons Island; (continued)

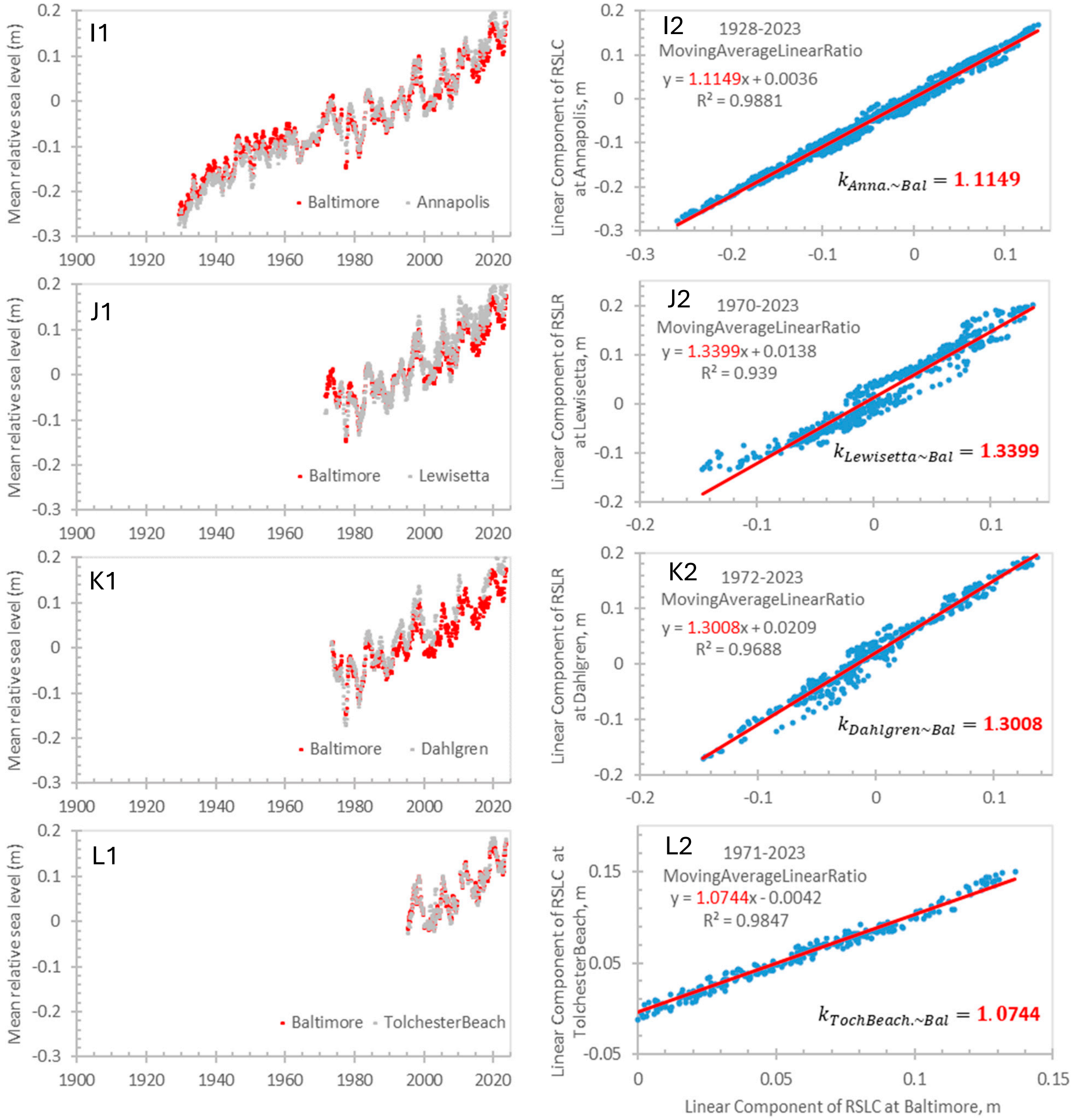

Supplementary Figure S1 (Continued) The correlation of reformed 11-month moving average relative sea levels between tide gauge Baltimore and each of 14 short-term tide gauges. I1, E2. Annapolis; **J1, J2.** Lewisetta; **K1, K2.** Dahlgren; **L1, L2.** Tolchester Beach.

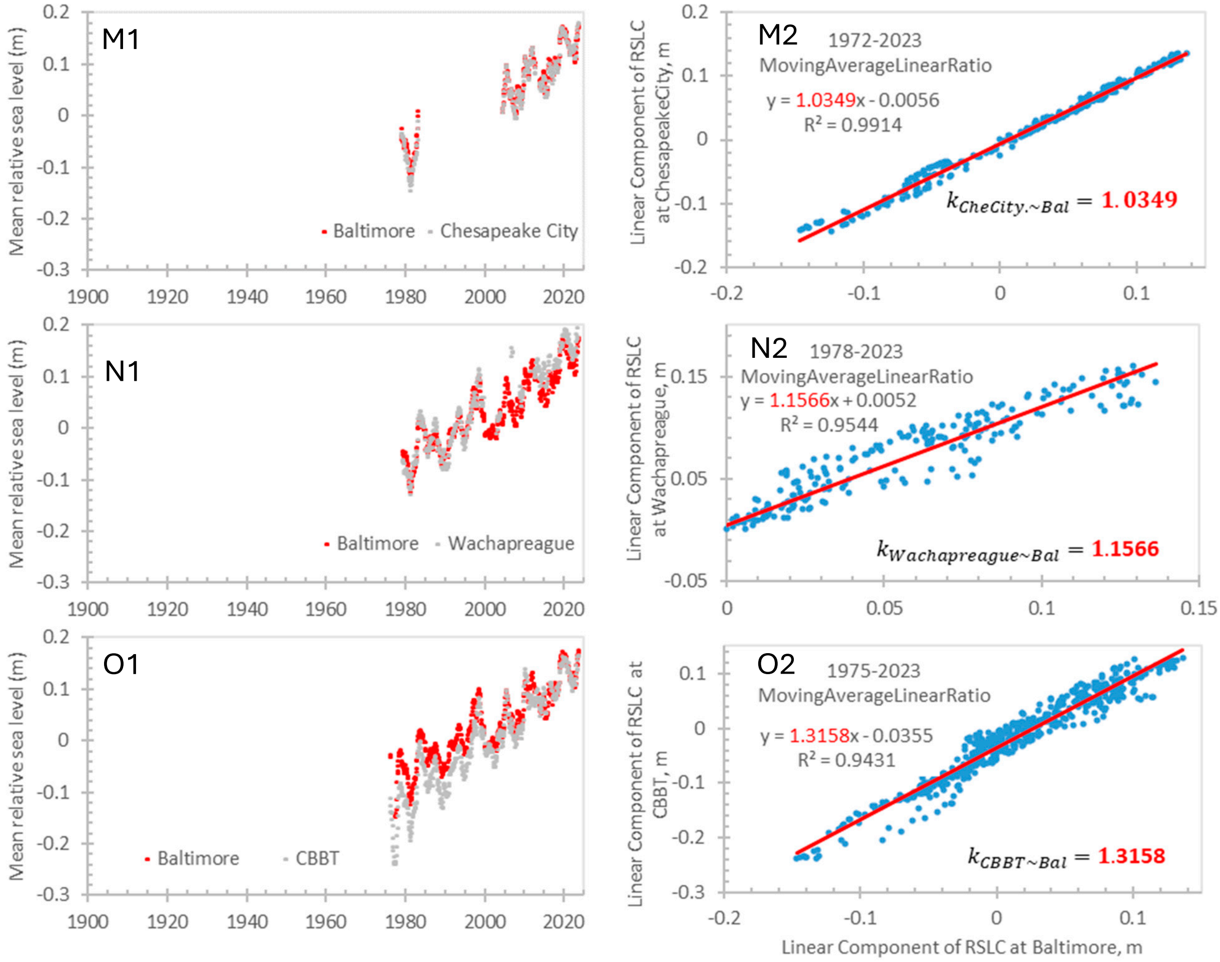

Supplementary Figure S1 (Continued) The correlation of reformed 11-month moving average relative sea levels between tide gauge Baltimore and each of other 14 tide gauges. M1, M2. Chesapeake City; N1, N2. Wachapreague; O1, O2. CBBT.

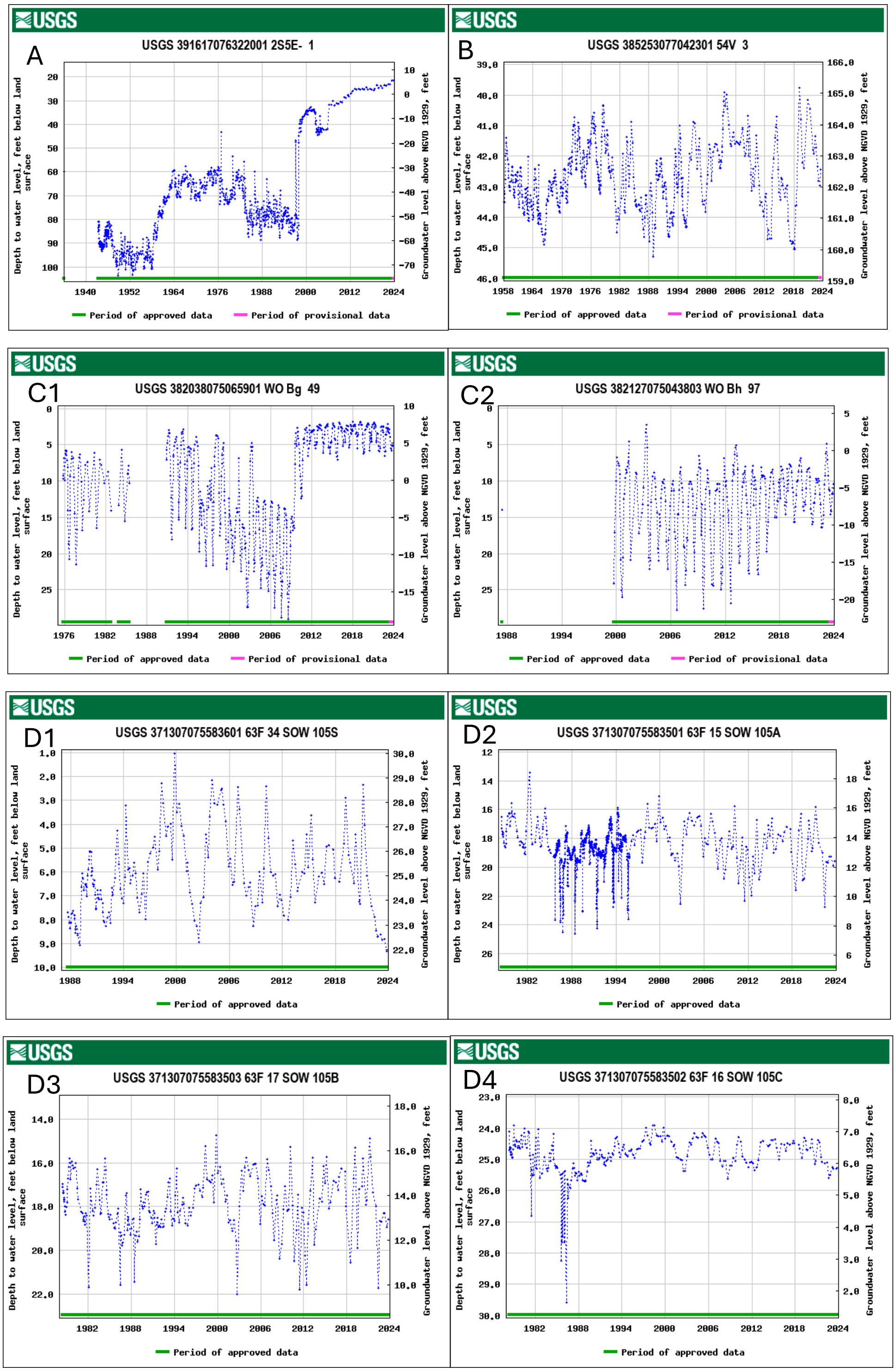

Supplementary Figure S2 The groundwater level time series of 8 wells near TGs Baltimore, Washington D.C., TG Ocean City and Kiptopeke, and graphs acquired from USGS National Water Information System (USGS, n.d.-b)**.** Subplot **A** is 2.5 km away from the TG Baltimore, subplot **B** is 5 km away from the TG Washington D.C., subplots **C1**, **C2** are 3 km away from the TG Ocean City, and subplots **D1** through **D4** are 7.5 km away from the TG Kiptopeke.

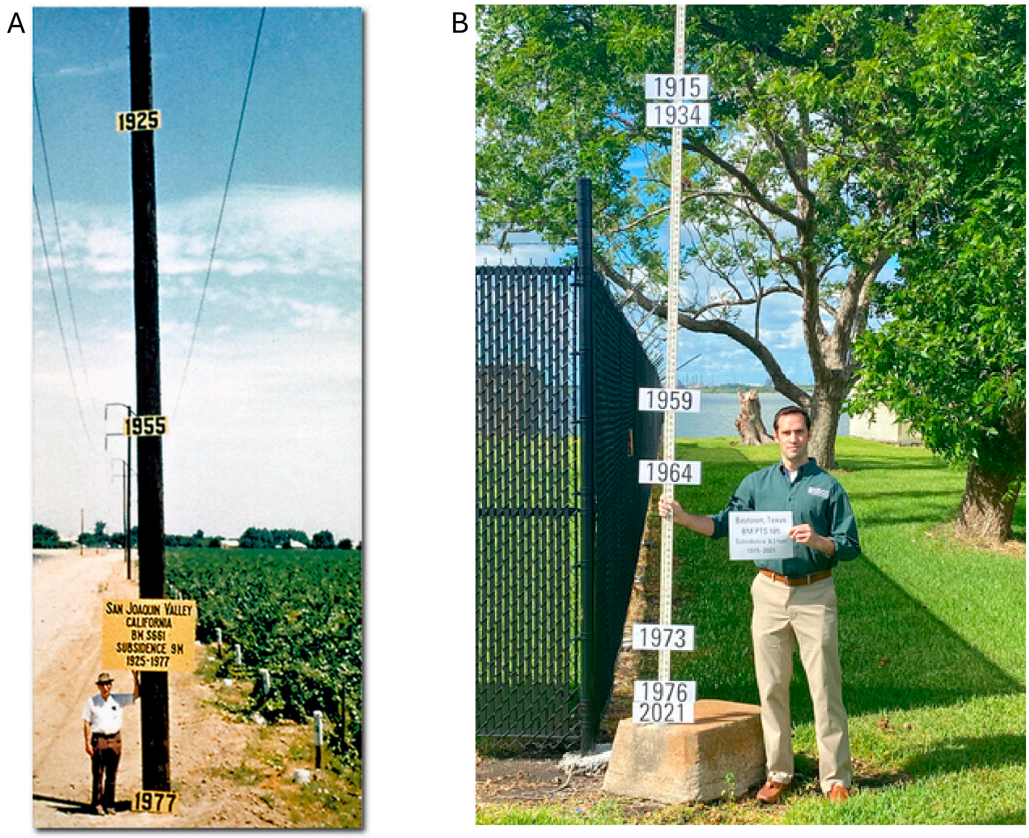

Supplementary Figure S3 Two examples of compaction subsidence (CS) in the United States. **A**. Primary consolidation subsidence (PCS) - Land subsidence in California - Approximate location of maximum subsidence in the United States identified by research efforts of Dr. Joseph F. Poland (pictured). Signs on pole show approximate altitude of land surface in 1925, 1955, and 1977. The site is in the San Joaquin Valley southwest of Mendota, California (By Water Science School 1977). **B**. USGS scientist, John Ellis, showing how much the land has subsided in the Houston area since 1915 (By Oklahoma-Texas Water Science Center 2022).

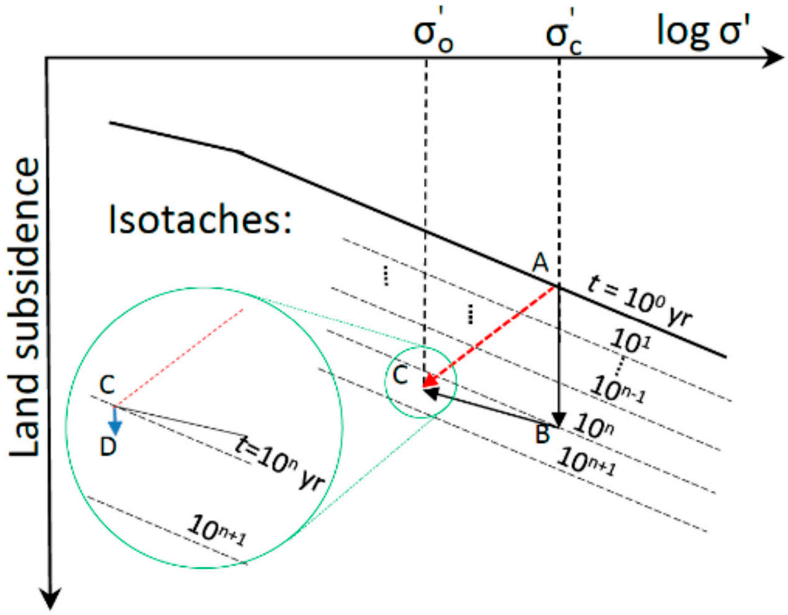

Supplementary Figure S4 Subsidence due to secondary consolidation (creep) subsidence (SCS) and historical changes in effective stress presented with a conceptual isotache model. Path A-B shows SCS due to 10^n year creep under a given overburden pressure σ_c'. Path B-C displays rebound due to an instant overburden removal at the age of 10n years and reduction of effective stress to σ_o' from σ_c'. Path A-C represents the combination of both the rebound and creep processes that may occur simultaneously. Path C-D at σ_o' shows insignificant SCS during 100 years (e.g., 1900 – 2000) from 10^n years to 10^n + 100 years [from [47]].

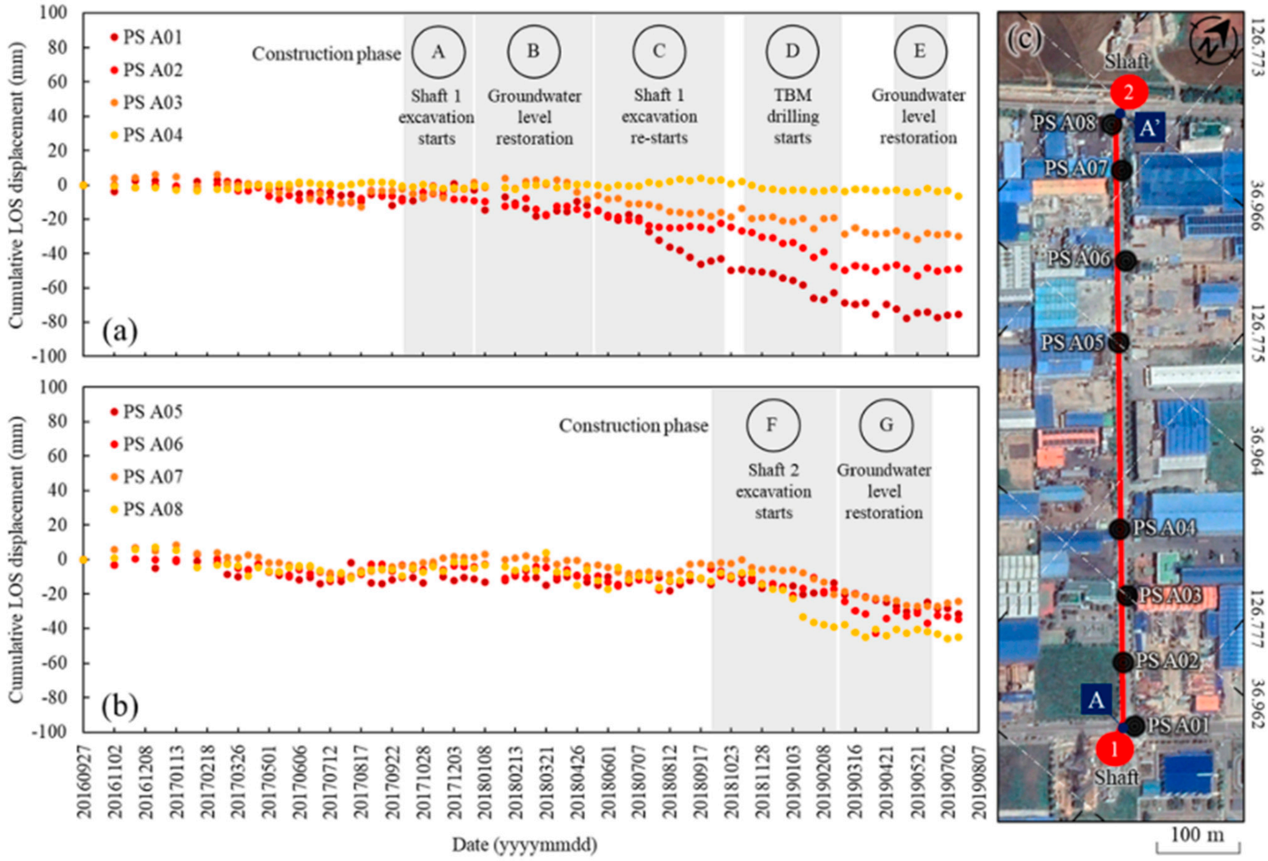

Supplementary Figure S5 Time series of cumulative line-of-sight (LOS) displacement for the selected persistent scatterer (PS) points along tunnel A-A' in Dangjin, Korea [48]**. (a)** PS A01-to-PS A04 and **(b)** PS A05-to-PS A08. Locations of PS points, vertical shafts, and tunnel route are shown in **(c)**.

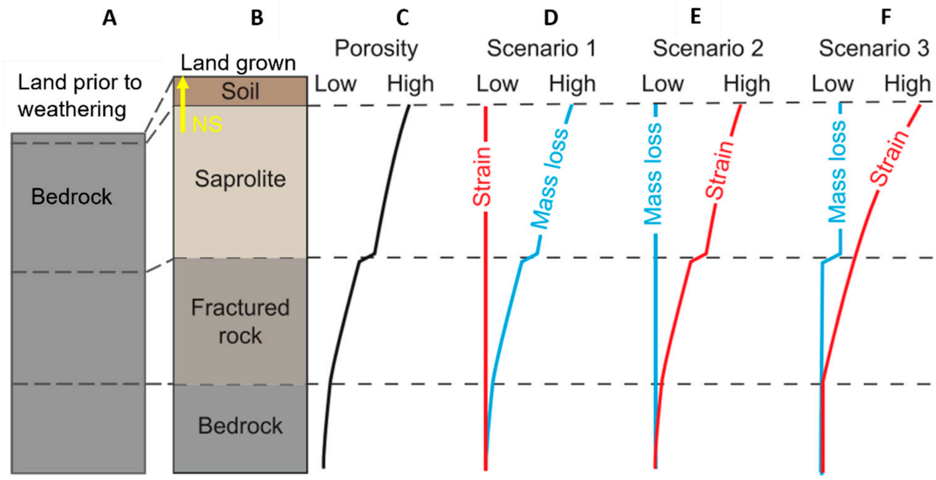

Supplementary Figure S6 Conceptual model of negative subsidence (NS) from land growth caused by vertical expansion of bedrock to soil+saprolite+fractured-rock due to weathering in Quaternary. (**A**) Bedrock profile prior to weathering; (**B**) The weathering profile consisting of the mobile soil layer, saprolite (which is weathered but retains the texture of underlying bedrock), fractured rock, and fresh bedrock at depth; (**C**) The increase in porosity with proximity to the top surface of saprolite such as landscape surface in mountains by erosion; (**D**) The increase in mass loss without strain; (**E**) The increase in strain without mass loss; and (**F**) The increase in mass loss and strain. (**B**) through (**E**) are from [50] with modification in **B**. NS rate would be about 0.005 mm/year for a 33.3 meter thick soil+saprolite+fractured-rock layer with an average porosity of 0.4 weathered from a 21.4 meter thick bedrock layer with an average porosity of 0.055 [88], which is insignificant in the human measurement period. If the soil+saprolite+fractured-rock layer, such as the one beneath a tide gauge, is submerged, the NS rate can be considered to be zero.

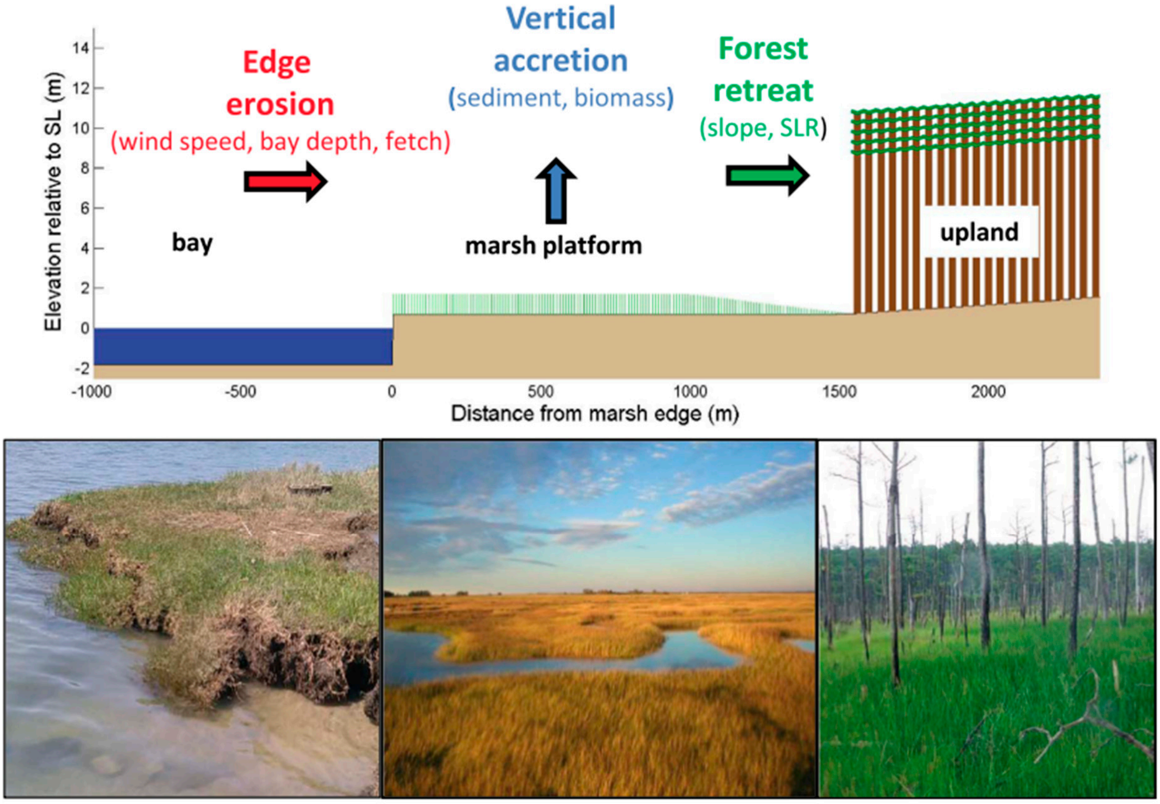

Supplementary Figure S7 Land loss due to erosion and land accretion due to sedimentation and biomass growth between subtidal, intertidal, and terrestrial ecosystems in coastal marshland [51].

Supplementary Figure S8 A photo of the surficial sediment. Surficial aquifer (Q^W) of weathered subcrop Chesapeake Group/Choptank Formation sandstone and siltstone (Miocene of Tertiary) at Calvert Cliffs (38.405039, -76.410392, 24 m high).